






A Novel SEIAISRD Model to Evaluate Pandemic Spreading

Hui Wei^{1,2}  and Chunyan Zhang^{1,2}  

¹ Department of Automation, College of Artificial Intelligence, Nankai University, Tianjin 300071, China

² Tianjin Key Laboratory of Intelligent Robotics, Nankai University, Tianjin 300071, China

zhcy@nankai.edu.cn

Abstract. Starting in late March 2021, several countries have been massively promoting vaccination, sparking a global debate on whether containment or suppression strategies response to COVID-19 remain necessary. To evaluate the potential impact of SARS-CoV-2 vaccines and control strategies, a data-driven, discrete-time compartmental model is developed, incorporating the unparalleled characteristics of the epidemic. This model is then calibrated to country-level reported active cases, accumulative recovered and deceased cases, as well as daily new cases. Indeed, this paper applies the calibrated model to reconstruct the transmission dynamics of the outbreak over time, especially after the emergence of various vaccines. The results, combined, demonstrate that the current vaccines appear to be insufficient to eliminate this disease, despite the increasing number of vaccinations, highlighting that such control strategies or restrictions are not supposed to be completely lifted across the world. Finally, there is no denying that the proposed model and framework can be readily extended to other countries, states, regions, or organizations.

Keywords: COVID-19 · Data-driven approach · Epidemiological model · Decision-making

1 Introduction

The ongoing COVID-19 epidemic, an international public health emergency caused by the novel coronavirus [18], has been posing unprecedented challenges to social economics, humanitarian rights, and healthcare systems around the world [4]. COVID-19 was officially declared a global pandemic by the World Health Organization on 11 March 2020 [21]. This epidemic, as of late October 2021, has spread rapidly to over 220 countries, causing more than 240 million accumulative confirmed cases and 4.9 million deaths, which thus be regarded as a more terrible pandemic compared to the Spanish flu. Among these countries, the most representative examples, affected by the epidemic, include such as

Supported by the National Natural Science Foundation of China under Grants 62073174, 62073175 and 91848203.

America with over 46 million cases and 763 thousand deaths, India with over 34 million cases and 450 thousand deaths, Brazil with over 21 million cases and 600 thousand deaths, England with over 8.9 million cases and 140 thousand deaths, as well as Russia with over 8.3 million cases and 235 thousand deaths, etc.

China is the first batch of countries to experience the challenge associated with the COVID-19 epidemic. From 23 January to 8 April 2020, the Chinese authority, by imposing a series of stringent lockdown measures or non-pharmaceutical interventions, successfully contained the large-scale outbreak of COVID-19 in Wuhan, the capital of Hubei province [15]. This control strategy, to date, results in less than 100 thousand confirmed cases and 4.7 thousand deaths for mainland China. Since then, these strategies such as enhanced testing, contact tracing, household quarantine, mask-wearing, and social distancing, etc., were successively followed by South Korea, Australia, Singapore, Denmark, and other countries [13]. Despite such rigorous requirements, those countries have successfully given evidence to the possibility of the aforementioned interventions for alleviating the spread of the outbreak. Such extreme strategies, nevertheless, may be able to interrupt temporarily the disease transmission, yet come at the price of tremendous economic losses or social destruction. In the countries that have curbed the initial outbreak of COVID-19, there is still a continued controversy over when to relax, where to be implemented, and how to reopen economic and social activities [6].

To help policy-makers to formulate optimal policies for restarting economic activity and normal social functioning, while avoiding a future resurgence of the outbreak, mathematical models are proved as a unique, yet efficient tool for this aim. Specifically, mathematical models can contribute profound insight for them into the potential impact of existing control strategies, as well as into the evaluation of possible governmental policies [1]. A typical example of the latter, for instance, is that some countries have experienced a thorough shift in defending the so-called “herd immunity” policies even without any interventions. This, to a large degree, can be contributed to the model developed by the Imperial College London that predicts extensive death tolls before achieving this intention. More incisive insights into the transmission dynamics of such large-scale pandemics can be benefited by using SIR- or SEIR-type compartmental models [22]. For the COVID-19 epidemic, several compartmental models have been flourished, considering the unparalleled characteristics of this epidemic such as asymptomatic infection, longer incubation period, and super-spreader event [10], etc., even incorporating post-epidemic interventions (e.g., distancing-like measures or quarantine scenarios) [11]. Those compartmental models have indicated that the disease transmission, through rapidly testing, quarantining and contact tracing, can be significantly interrupted [2]. Alternatively, most of them were established with incomplete data, affecting the confidence in produced results for driving public health policy [5]. Validating COVID-19 modelling predictions is thus of great importance.

So far, for public health policies imposed in severely affected countries, it has been characterized by insufficient adherence to social distancing, logistic chal-

challenges for implementing large-scale contact-tracing, along with deficient detecting kits and relevant supplies [9]. Recent researches reveal that increased detecting and contact-tracing efficiency may contribute to reducing the significantly increasing number of accumulative confirmed cases and deaths in America, England, Italy, and other countries [20]. Several modelling researches have looked at the spatial dynamics of the outbreak and its evolution in the region at the state level [17] but, to our knowledge, limited work has focused on the functions of diverse containment and suppression strategies [19]. Comprehending the degree to which these strategies, such as enhanced detecting, contact tracing and quarantining, local lockdown, as well as social distancing, etc., influence locally the disease transmission is fundamental for predicting and preventing second or even multiple resurgences of the epidemic [8]. This, in return, will promote the optimization of these strategies to alleviate the harmful economic burden caused by COVID-19, while developing energetically effective vaccines and associated therapeutics. Most modelling researches, however, were gained under a common assumption, that is, without an effective vaccine. Among those researches, few took into account the impact of vaccines and their relevant vaccination information. This has inevitably sparked a debate for us on whether such control strategies are necessary, and on how to release them while escaping from future outbreaks, after the emergency of various vaccines.

In this work, our primary purpose is to further explore the evolution of the COVID-19 epidemic over time in each stage but, more importantly, after the emergency of various vaccines. Specifically, a data-driven, discrete-time compartmental model, named SEIAISRD, is developed, incorporating the aforementioned characteristics of COVID-19, even combining the effectiveness of various vaccines and relevant vaccination information. The model parameters, using the extended Kalman filter algorithm, are practically calibrated to country-level reported active cases, accumulative recovered and deceased cases, as well as daily new cases from 24 January 2020 to 22 October 2021. Additionally, this calibrated model is then applied to evaluate the potential impact of current SARS-CoV-2 vaccines and control strategies implemented in each country, presenting a data-fitting comparison between the estimated and reported cases. Finally, this model, by just recalibrating and recalculating the assumed values for model parameterization, can be extended or readily applicable to reevaluate the current situation responding to the epidemic for those representative countries, such as America, India, England, China, and Brazil, etc.

2 Methods

2.1 The SEIAISRD Model

This paper has modified the generalized *SIR* or *SEIR* model to capture the evolution of COVID-19 over time in each stage, especially after the emergence of various vaccines. The SEIAISRD model, combining the unprecedented characteristics of this epidemic, assumes that susceptible individuals (S), to a certain potential, can become exposed individuals (E), through any contact with the

SARS-COV-2 virus. After passing for an incubation period, E , who is in latent yet non-infectious stage, can either be transmitted to asymptomatic infected (I_A) or symptomatic infected (I_S). Finally, the infected individuals will be transmitted to the removed compartments, identifying recovered (R) or deceased (D) individuals. Note that, I_A will be recovered following hospitalization, whereas I_S , especially those with severe symptoms, are faced with the risk of death in the initial outbreak. The flow diagram of this model is schematically described in Fig. 1. To balance fidelity and identifiability of the calibrated model, it is reasonable for us to assume that all infected cases are effectively tested or isolated, and thus unavailable for transmitting the virus.

The proposed model, describing, respectively, the dynamics of the following six compartments (e.g., S , E , I_A , I_S , R and D), is given by:

$$\frac{dS}{dt} = -\frac{(1-\alpha)\beta S(I_A + I_S)}{N}, \quad (1)$$

$$\frac{dE}{dt} = \frac{(1-\alpha)\beta S(I_A + I_S)}{N} - \epsilon E, \quad (2)$$

$$\frac{dI_A}{dt} = \rho_1 \epsilon E - \gamma_1 I_A, \quad (3)$$

$$\frac{dI_S}{dt} = \rho_2 \epsilon E - (\gamma_2 + \mu) I_S, \quad (4)$$

$$\frac{dR}{dt} = \gamma_1 I_A + \gamma_2 I_S, \quad (5)$$

$$\frac{dD}{dt} = \mu I_S, \quad (6)$$

where β and γ denote, respectively, the infection rate and the recovery rate. Among which, γ_1 is the recovery rate of asymptomatic infected individuals (I_A), yet γ_2 is that of symptomatic infected individuals (I_S). $\alpha \in [0, 1]$ is a parameter modelling the effectiveness of SARS-COV-2 vaccines. The remaining parameters include such as the mean exposed period ϵ (day^{-1}), the case fatality rate μ , as well as the proportion of exposed individuals (E) proceeding to asymptomatic (or symptomatic) infections ρ_1 (or ρ_2), obviously, $\rho_1 + \rho_2 = 1$. Remark that since this epidemic is transmitted by a person-to-person pattern, and no evidence showing that parasite vector or environmental parameters have immensely influenced its infection rate, it thus is assumed that β is the same for all countries. Besides, the actual population of the country N can be divided into the aforementioned six compartments and satisfies

$$N = S + E + I_A + I_S + R + D. \quad (7)$$

Of note, the actual epidemic data of COVID-19 for each country [12], collected by the Johns Hopkins CSSE Repository, includes the following reported cases, such as the active cases, accumulative recovered and deceased cases, as well as daily new confirmed cases. To fit accurately the proposed model to these

data, a discrete-time augmented SEIAISRD model, by augmenting the infection rate β and daily new confirmed individuals (C) as additional state variables, can be obtained as follows:

$$S(k+1) = S(k) - \frac{(1-\alpha)\beta(k)S(k)(I_A(k) + I_S(k))\Delta t}{N} + \omega_1(k), \quad (8)$$

$$E(k+1) = E(k) + \frac{(1-\alpha)\beta(k)S(k)(I_A(k) + I_S(k))\Delta t}{N} - \epsilon E(k)\Delta t + \omega_2(k), \quad (9)$$

$$I_A(k+1) = I_A(k) + \rho_1 \epsilon E(k)\Delta t - \gamma_1 I_A(k)\Delta t + \omega_3(k), \quad (10)$$

$$I_S(k+1) = I_S(k) + \rho_2 \epsilon E(k)\Delta t - (\gamma_2 + \mu) I_S(k)\Delta t + \omega_4(k), \quad (11)$$

$$R(k+1) = R(k) + \gamma_1 I_A(k)\Delta t + \gamma_2 I_S(k)\Delta t + \omega_5(k), \quad (12)$$

$$D(k+1) = D(k) + \mu I_S(k)\Delta t + \omega_6(k), \quad (13)$$

$$C(k+1) = C(k) + (\gamma_1 + \gamma_2 + \mu)(I_A(k) + I_S(k))\Delta t - C(k)\Delta t + \omega_7(k), \quad (14)$$

$$\beta(k+1) = \beta(k) + \omega_8(k), \quad (15)$$

where Δt is the simulation time step (this paper sets $\Delta t = [0.1, 0.001]$). The White Gaussian noise $\omega(k) = [\omega_1(k) \ \omega_2(k) \ \cdots \ \omega_8(k)]^T$ is utilized to express model uncertainty and is assumed to be uncorrelated. Extending a parameter to a new state variable, note that, is an ordinary measure when estimating model parameters using the extended Kalman filter (EKF) (more details are illustrated on page 422 of [16]).

2.2 Estimating the Effective Reproduction Number

The effective reproduction number, R_t , is defined by the average number of second-generation infected cases (e.g., asymptomatic or symptomatic infected cases) transmitted from a single infected individual at a certain time t [14]. It is still unclear whether the individuals recovered from the COVID-19 epidemic will be re-infected, whereas initial evidence reveals that this is little possibility [23]. This paper thus assumes that only a single infected case relevant to this epidemic may occur to any single individual. As reminded above, R_t , as a qualitative index, is often used to capture the transmission dynamics of the epidemic. For example, as $R_t > 1$, the epidemic will spread rapidly among the population, whereas the epidemic will gradually disappear for $R_t < 1$. Accordingly, it presents a quantitative tool of whether further control efforts or interventions are necessary to curtail the spread of COVID-19. Based on the series of daily new confirmed cases, R_t is considered here to be the source of the general update equation during a birth process, and defined as

$$R_t = \frac{S(t)}{N} \beta (1 - \alpha) \left(\frac{\rho_1}{\gamma_1} + \frac{\rho_2}{\gamma_2 + \mu} \right), \quad (16)$$

where the term $S(t)/N$ is utilized to compensate the reduction in susceptible individuals, and then, multiplies by the infected risk of each contact for infected

individuals and their untraced contacts, $\beta(1 - \alpha)$, and their mean infection period, $\left(\frac{\rho_1}{\gamma_1} + \frac{\rho_2}{\gamma_2 + \mu}\right)$. This may be, respectively, explained by the contribution of asymptomatic infected (I_A), $\frac{S(t)}{N}\beta(1 - \alpha)\frac{\rho_1}{\gamma_1}$, and symptomatic infected (I_S), $\frac{S(t)}{N}\beta(1 - \alpha)\frac{\rho_2}{\gamma_2 + \mu}$.

In this section, the extended Kalman filter (EKF) is adopted by us to estimate dynamically the effective reproduction number. For brevity of the reading pubic, an augmented state vector is defined as $x(k + 1) = [S(k + 1) \ E(k + 1) \ I_a(k + 1) \ I_s(k + 1) \ R(k + 1) \ D(k + 1) \ C(k + 1) \ \beta(k + 1)]^T$, such that the discrete-time augmented SEIAISR model (8)-(15) can be modified as $x(k + 1) = f(x(k)) + \omega(k)$. Since then, let us regard $\hat{x}(k)$ as the estimated vector of $x(k)$ from the EKF. $f(x(k)) = f(\hat{x}(k)) + J_f(\hat{x}(k))(x(k) - \hat{x}(k))$ is obtained by applying first-order Taylor series expansion to f at $\hat{x}(k)$, among which, the Jacobian matrix is $J_f(\hat{x}(k))$ described by

$$J_f(\hat{x}(k)) = \begin{bmatrix} J_{11} & 0 & J_{13} & J_{14} & 0 & 0 & 0 & J_{18} \\ J_{21} & J_{22} & J_{23} & J_{24} & 0 & 0 & 0 & J_{28} \\ 0 & \rho_1 \varepsilon \Delta t & 1 - \gamma_1 \Delta t & 0 & 0 & 0 & 0 & 0 \\ 0 & \rho_2 \varepsilon \Delta t & 0 & J_{44} & 0 & 0 & 0 & 0 \\ 0 & 0 & \gamma_1 \Delta t & \gamma_2 \Delta t & 1 & 0 & 0 & 0 \\ 0 & 0 & 0 & \mu \Delta t & 0 & 1 & 0 & 0 \\ 0 & 0 & J_{73} & J_{74} & 0 & 0 & 1 - \Delta t & 0 \\ 0 & 0 & 0 & 0 & 0 & 0 & 0 & 1 \end{bmatrix}, \quad (17)$$

where

$$J_{11}(\hat{x}(k)) = 1 - \frac{(1 - \alpha)\beta(k)(I_A(k) + I_S(k))\Delta t}{N}, \quad (18)$$

$$J_{13}(\hat{x}(k)) = J_{14}(\hat{x}(k)) = -\frac{(1 - \alpha)\beta(k)S(k)\Delta t}{N}, \quad (19)$$

$$J_{18}(\hat{x}(k)) = -\frac{(1 - \alpha)S(k)(I_A(k) + I_S(k))\Delta t}{N}, \quad (20)$$

$$J_{21}(\hat{x}(k)) = \frac{(1 - \alpha)\beta(k)(I_A(k) + I_S(k))\Delta t}{N}, \quad (21)$$

$$J_{22}(\hat{x}(k)) = 1 - \epsilon \Delta t, \quad (22)$$

$$J_{23}(\hat{x}(k)) = J_{24}(\hat{x}(k)) = \frac{(1 - \alpha)\beta(k)S(k)\Delta t}{N}, \quad (23)$$

$$J_{28}(\hat{x}(k)) = \frac{(1 - \alpha)S(k)(I_A(k) + I_S(k))\Delta t}{N}, \quad (24)$$

$$J_{44}(\hat{x}(k)) = 1 - (\gamma_2 + \mu)\Delta t, \quad (25)$$

$$J_{73}(\hat{x}(k)) = J_{74}(\hat{x}(k)) = (\gamma_1 + \gamma_2 + \mu)\Delta t. \quad (26)$$

Further details of the extended Kalman filter applied to the SIR or SEIR-type model are illustrated in [16].

2.3 Data-Fitting and Sensitivity Analysis

Real-world reported cases, originating from 24 January 2020 to 22 October 2021, have been used to fit the SEIAISRD model. All data-fitting analyses have been performed with a MATLAB optimization toolbox using the extended Kalman filter. This optimization algorithm, given all inputs that vary within the ranges found from several researches, is verified as the optimal solution. Infected initial inputs have been determined from reported active cases, accumulative recovered, and deceased cases, whereas the remaining initial inputs could vary during the optimization process. To describe the inherent uncertainty of COVID-19, consequently to demonstrate the impact of combined control strategies and vaccines, the aforementioned results are the average outputs by running over 50 independent repetitive simulations. Specifically, the model parameters α , β , ϵ , γ_1 , γ_2 , μ together with the initial inputs have been chosen, incorporating a $\pm 20\%$ maximum variation from their normal values. It is suggested that the proposed model and algorithm are robust to several parameter variations, demonstrating the feasibility to curtail this epidemic and expandability to be extended to other countries across the world. Estimated 95% confidence intervals have taken the 1% perturbations of uniform distribution into account, to assess the corresponding confidence in the results, and finally to compare the fitting results with actual reported cases, such as active cases, accumulative recovered and deceased cases, as well as daily new confirmed cases. COVID-19 active cases, accumulative recovered and deceased cases, daily new confirmed cases, as well as vaccination information for mainland China, are obtained by the National Health Commission of the People's Republic of China [7] and are available at <http://www.nhc.gov.cn/>. Whereas for the representative countries (e.g., America, India, Brazil, Russia, France, Turkey, England, Argentina, Italy, and Colombia), collected by Johns Hopkins CSSE Repository, can be available at <https://github.com/CSSEGISandData/COVID-19>.

3 Results

3.1 Model Formulation and Validation

To capture the evolution of the ongoing COVID-19 epidemic over time in each stage, especially after the emergence of various vaccines, a data-driven, discrete-time compartmental SEIAISRD model is performed to evaluate the impact of current SARS-CoV-2 vaccines and control strategies for several representative countries (such as China, America, India, Brazil, Russia, France, Turkey, England, Argentina, Italy, and Colombia). The SEIAISRD model, combining the unprecedented characteristics of COVID-19, main includes the following compartments: susceptible, S ; exposed, E ; asymptomatic infected, I_A ; symptomatic infected, I_S ; recovered, R ; and deceased, D ; described schematically in Fig. 1. This is an epidemiological modelling tool that can reconstruct the transmission dynamics of COVID-19 within a population. As shown in Fig. 1, this model assumes that susceptible individuals (S) become exposed individuals (E), to a

certain probability, through contact with any of the infected compartments (e.g., asymptomatic infected (I_A) or symptomatic infected (I_S), which means that the exposed individuals (E) are in latent, yet non-infectious stage. After passing for a mean exposed period, the exposed individuals (E) are then transitioning to asymptomatic infected (I_A) or symptomatic infected (I_S). Finally, the infected individuals will be transitioning to the removed compartments, identifying recovered (R) or deceased (D) individuals.

Table 1. Calibrated model parameters for the SEIAISR model.

Parameter	Definition
N	Population size of the corresponding country
α	The effectiveness of SARS-COV-2 vaccine
β	Transmission rate
ϵ	Mean exposed period
ρ_1	Proportion of exposed transitioning to asymptomatic infected (I_A)
ρ_2	Proportion of exposed transitioning to symptomatic infected (I_S)
γ_1	Recovery rate of asymptomatic infected (I_A)
γ_2	Recovery rate of symptomatic infected (I_S)
μ	The case fatality rate

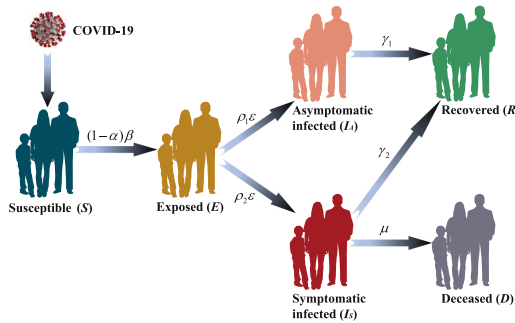


Fig. 1. Schematic diagram of the SEIAISR model structure. The SEIAISR, a date-driven, discrete-time compartmental model, is presented to reconstruct the transmission dynamics of the ongoing COVID-19 epidemic after the emergency of various vaccines. This model, combining the unprecedented characteristics of COVID-19, includes mainly six compartments, such as susceptible (S), exposed (E), asymptomatic infected (I_A), symptomatic infected (I_S), recovered (R), and deceased (D).

As regards validation, the model parameters, using the extended Kalman filter algorithm, are calibrated to country-level reported active cases, recovered cases, deceased cases, and daily new cases from 24 January 2020 to 22

October 2021. Estimating all the parameters regarding each country allows us to not only precisely fit the reported COVID-19 cases, but also to describe the diverse country situations and the disparate impacts of government policies aiming to contain this epidemic spread for those selected countries right now. Calibrated model parameters are highlighted in Table 1. A detailed description of the SEIAISRD model consideration, parameterization, and sensitivity analysis are further explained in Methods. Besides, further details on the real-world reported cases and vaccination information for each country can be found at <https://github.com/CSSEGISandData/COVID-19>, as collected by Johns Hopkins CSSE Repository [12].

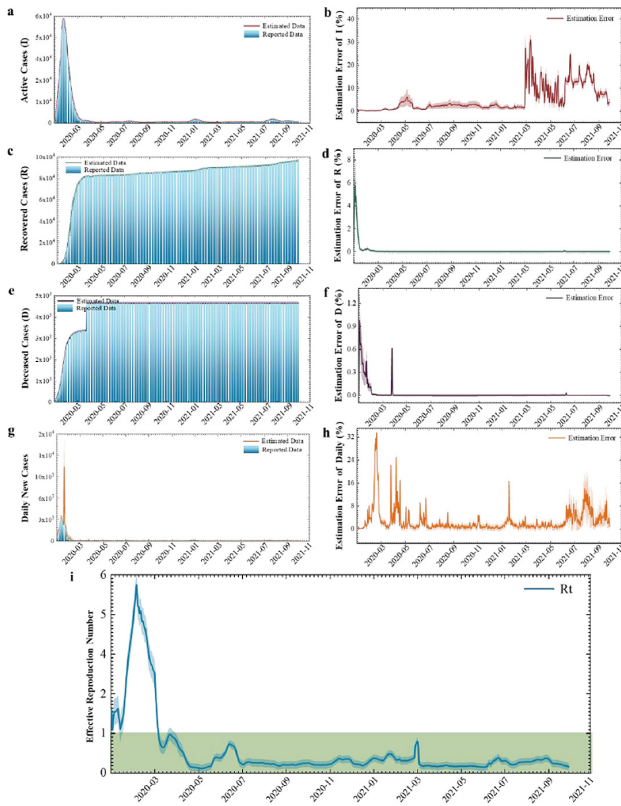


Fig. 2. Real-time modelling and fitting results of COVID-19 for mainland China: (a) Active cases; (b) Estimation error of active cases; (c) Accumulative recovered cases; (d) Estimation error of accumulative recovered cases; (e) Accumulative deceased cases; (f) Estimation error of accumulative deceased cases; (g) Daily new confirmed cases; (h) Estimation error of Daily new confirmed cases. (i) Effective reproduction number R_t .

3.2 Case Studies for the Representative Countries

As all we know, China is the first batch of the countries to experience the challenge caused by COVID-19, a case study on transmission dynamics of the epidemic for mainland China is thus investigated. Unlike most previous researches, this paper underscores the evolution of this epidemic over time in each stage, especially after the emergence of various vaccines. To this aim, the model parameters are calibrated to match the crucial characteristics of the reported COVID-19 cases. The results, as described in Fig. 2, show numerical simulations of real-time modelling and data fitting of COVID-19 for mainland China, including a comparative analysis of the relative Root Mean Square Errors (for brevity, it is next referred to as estimation errors) between the corresponding estimated and real-world reported cases. Among which, Fig. 2a, c, e, and g show, respectively, the evolution of the estimated active cases, accumulative recovered and deceased cases, as well as daily new confirmed cases. Figure 2b, d, f, and h represent, respectively, the estimation errors between the corresponding estimated and reported cases (e.g., active cases, accumulative recovered cases and deceased cases, as well as daily new confirmed cases), hinting at this observation is in a great agreement with recent reports of COVID-19 for mainland China. It is worth stressing that, the fluctuations in the estimation errors of active cases and daily new confirmed cases (e.g., Fig. 2b and Fig. 2h), to a large extent, are related to the abroad inputs of asymptomatic infected cases. In doing so, it is confirmed that the SEIAISR model has correctly predicted the active cases, daily new confirmed cases, as well as accumulative recovered and deceased cases.

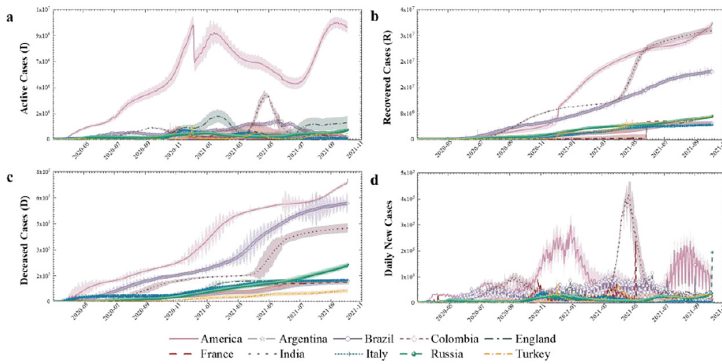


Fig. 3. Real-time fitting results of COVID-19 for several representative countries: (a) Active cases; (b) Accumulative recovered cases; (c) Accumulative deceased cases; (d) Daily new confirmed cases. Those selected countries are chosen from the top ten countries regarding accumulative confirmed cases, such as America, India, France, Turkey, England, Argentina, Italy, and Colombia in order. The shaded error bands denote, respectively, 95% confidence intervals of the corresponding mean by running over 50 independent repetitive experiments. For easy comparison, raw data, represented by this plot, are selected from 1 March 2020 to 22 October 2021.

Furthermore, the time-varying effective reproduction number for mainland China, presented in Fig. 2i, is estimated by using the SEIAISRD model together with the extended Kalman filter, indicating that this epidemic keeps to a typical trajectory. It is well known that the effective reproduction number, R_t , is the average number of second-generation infected cases (e.g., asymptomatic or symptomatic infected cases) transmitted from a single infected individual at a certain time t [14]. Generally speaking, R_t , as a qualitative index, is often used to describe the real-time transmission dynamics of epidemic disease. For example, as $R_t > 1$, the epidemic will spread rapidly among the population, whereas the epidemic will gradually disappear for $R_t < 1$. It is worth stressing that the SEIAISRD model would be readily extended to other regions, states or countries. To this end, the representative examples of the countries, which belong to the top ten countries regarding accumulative confirmed cases (e.g., America, India, Brazil, Russia, France, Turkey, England, Argentina, Italy, and Colombia), are chosen to demonstrate the applicability of the proposed model. After which, most model parameters remain constant except for the effectiveness of the SARS-COV-2 vaccine α . The results, as shown in Figs. 3, 4, display the evolution of COVID-19 after the emergence of various vaccines for those selected countries, incorporating a comparative analysis of the estimation errors between the corresponding estimated and real-world reported cases.

Figure 3 implies the real-time data-fitting results of several representative countries, such as America, India, Brazil, Russia, France, Turkey, England, Argentina, Italy, and Colombia. Of which, Fig. 3a, b, c, and d demonstrate that the proposed model can predict, respectively, the estimated active cases, accumulative recovered cases, accumulative deceased cases, and daily new confirmed cases for those selected countries, with real-world reported cases falling within its 95% confidence intervals. The results expose that, under current non-pharmaceutical interventions and SARS-COV-2 vaccines, this disease can not be thoroughly eliminated. Even though the increasing contact tracing and social distancing, they are still experiencing an increase in reported active, accumulative deceased, and daily new confirmed cases. France, Italy, and Brazil, for instance, may experience a continued increase in active cases within the following periods (Fig. 3a). America, Brazil, and India, on average, result in a sustained increase in accumulative deceased cases since the outbreak of this epidemic, whereas India, especially, has experienced an exponential increase since 1 April 2021 (Fig. 3c).

Bringing down and keeping up $R_t < 1$ is essential to mitigate the spread of the ongoing COVID-19 epidemic. The results, obtained systematically from Fig. 4, evaluate the potential of preserving $R_t < 1$ for those representative countries under current non-pharmaceutical interventions and SARS-COV-2 vaccines. It is therefore predicted that for the remaining countries (e.g., America, India, Brazil, Russia, France, Turkey, England, and Colombia) except Italy and Argentina, under the existing interventions and vaccinations coverage rate, curbing this epidemic appears to be impossible without additional control efforts, as the effective reproduction numbers are still insufficient to reduce and preserve $R_t < 1$. The Indian authority, for example, has ignored the warnings of scientists and

relaxed a series of quarantine measures starting in middle March 2021, causing people not strictly comply with quarantine rules, such as mask-wearing and social distancing [3]. This, on average, results in the peaks of 3,737,715 active cases (95% CI: 3,735,337-3,740,093), 453,704 accumulative deceased cases (95% CI: 453,641-453,767), and 406441 daily new confirmed cases (95% CI: 405,405–407,477) as of 22 October 2021. The aforementioned results, additionally, should not be regarded as the optimized interventions combining all possible model parameters, but rather as a distinct assessment of current situations for curtailing this epidemic around the world.

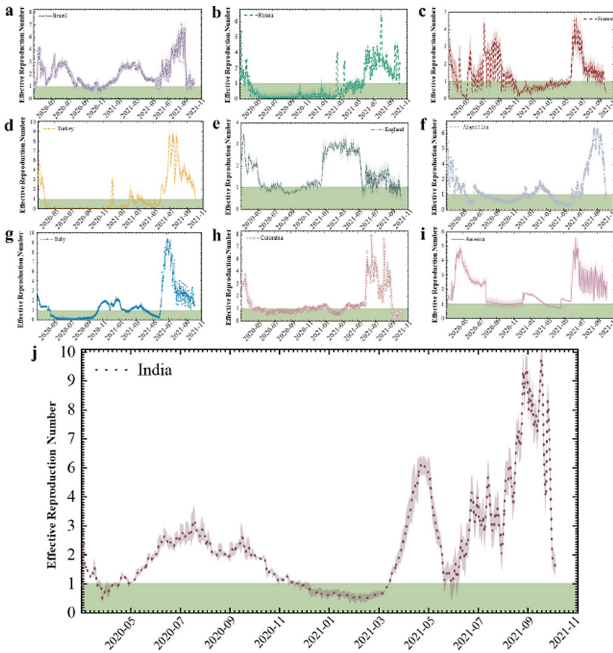


Fig. 4. Time-varying effective reproduction number R_t for several representative countries: (a) Brazil; (b) Russia; (c) France; (d) Turkey; (e) England; (f) Argentina; (g) Italy; (h) Colombia; (i) America; (j) India. Those selected countries are chosen from the top ten countries regarding accumulative confirmed cases, such as America, India, Brazil, Russia, France, Turkey, England, Argentina, Italy, and Colombia in order. The green rectangular region indicates $R_t < 1$. The shaded error bands denote, respectively, 95% confidence intervals of the corresponding mean by running over 50 independent repetitive experiments. For easy comparison, raw data, represented by this plot, are selected from 1 March 2020 to 22 October 2021. (Color figure online)

4 Conclusion

This paper has reconstructed the transmission dynamics of COVID-19 over time in each stage for mainland China. The mathematical model, SEIAISRD, has been calibrated to real-world epidemic reported cases, accounting for non-detected infections, symptomatic-asymptomatic infections distinction, variant-dependent transmission rates, the effectiveness of various vaccines, as well as the remaining epidemiological parameters. A considerable calibration result is the proportion of asymptomatic infections found to be 1.2% of that of the reported infected cases, yet its recovery rate found to be twice as high among symptomatic infections. Alternatively, in countries faced with advanced over-dispersion and super-spreader characteristics during the ongoing COVID-19 outbreak, the effective reproduction number, to a large degree, will be experiencing fluctuations as the asymptomatic/symptomatic infected cases decreases. This is more possible to help explain the case for countries with lower posterior values related to dispersion parameters, such as Brazil, Russia, France, England, America, Italy, as well as India, etc. It should, however, be worth stressing that the estimation errors for India continue to be fluctuating, compared to the remaining nine countries. It is well known that India is a developing country with a large population, and its healthcare resources, including the number of vaccinations, all fall behind those of developed countries. This phenomenon is thus extremely unreasonable. To sum up, it is imperative for us to conclude that there are some uncertainties in the actual epidemic data released by India. Future researches tend to address further aspects as, yet may not be limited to, exploring how the heterogeneity of the social contact network can affect the transmission dynamics of the outbreak, as well as declining uncertainty around the modelling approaches in different countries, regions, or crowds.

References

1. Aleta, A., et al.: Modelling the impact of testing, contact tracing and household quarantine on second waves of Covid-19. *Nature Hum. Behav.* **4**(9), 964–971 (2020)
2. Anderson, R.M., Heesterbeek, H., Klinkenberg, D., Hollingsworth, T.D.: How will country-based mitigation measures influence the course of the Covid-19 epidemic? *Lancet* **395**(10228), 931–934 (2020)
3. Asrani, P., Eapen, M.S., Hassan, M.I., Sohal, S.S.: Implications of the second wave of Covid-19 in India. *Lancet Respir. Med.* **9**(9), e93–e94 (2021)
4. Bastani, H., et al.: Efficient and targeted Covid-19 border testing via reinforcement learning. *Nature* **599**(7883), 108–113 (2021)
5. Block, P., et al.: Social network-based distancing strategies to flatten the Covid-19 curve in a post-lockdown world. *Nat. Hum. Behav.* **4**(6), 588–596 (2020)
6. Brauner, J.M., et al.: Inferring the effectiveness of government interventions against Covid-19. *Science* **371**(6531) (2021)
7. N.H.C.: Covid-19 prevention and control: vaccination information, People’s Republic of China. http://www.nhc.gov.cn/xcs/yqjzqk/list_gzbd.shtml (2021)
8. Chiu, W.A., Fischer, R., Ndeffo-Mbah, M.L.: State-level needs for social distancing and contact tracing to contain Covid-19 in the United States. *Nat. Hum. Behav.* **4**(10), 1080–1090 (2020)

9. Collins, F.S.: Covid-19 lessons for research (2021)
10. Contreras, S., et al.: The challenges of containing SARS-CoV-2 via test-trace-and-isolate. *Nat. Commun.* **12**(1), 1–13 (2021)
11. Della Rossa, F., et al.: A network model of Italy shows that intermittent regional strategies can alleviate the Covid-19 epidemic. *Nat. Commun.* **11**(1), 1–9 (2020)
12. Dong, E., Du, H., Gardner, L.: An interactive web-based dashboard to track Covid-19 in real time. *Lancet. Infect. Dis* **20**(5), 533–534 (2020)
13. Gibney, E.: Whose coronavirus strategy worked best? scientists hunt most effective policies. *Nature* **581**(7806), 15–17 (2020)
14. Guerra, F.M., et al.: The basic reproduction number (r_0) of measles: a systematic review. *Lancet. Infect. Dis* **17**(12), e420–e428 (2017)
15. Hao, X., Cheng, S., Wu, D., Wu, T., Lin, X., Wang, C.: Reconstruction of the full transmission dynamics of Covid-19 in Wuhan. *Nature* **584**(7821), 420–424 (2020)
16. Hasan, A., Putri, E.R., Susanto, H., Nuraini, N.: Data-driven modeling and forecasting of Covid-19 outbreak for public policy making. *ISA transactions* (2021)
17. Hoertel, N., et al.: A stochastic agent-based model of the SARS-CoV-2 epidemic in France. *Nat. Med.* **26**(9), 1417–1421 (2020)
18. Hsiang, S., et al.: The effect of large-scale anti-contagion policies on the Covid-19 pandemic. *Nature* **584**(7820), 262–267 (2020)
19. Li, Z., et al.: Active case finding with case management: the key to tackling the Covid-19 pandemic. *Lancet* **396**(10243), 63–70 (2020)
20. Monti, M., Torbica, A., Mossialos, E., McKee, M.: A new strategy for health and sustainable development in the light of the Covid-19 pandemic. *Lancet* **398**(10305), 1029–1031 (2021)
21. Organization, W.H.: Coronavirus disease 2019 (Covid-19) situation report-71 (world health organization, accessed 31 Mar 2020). http://www.who.int/docs/default-source/coronaviruse/situation-reports/20200331-sitrep-71-covid-19.pdf?sfvrsn=4360e92b_8 (2020)
22. Rockx, B., et al.: Comparative pathogenesis of Covid-19, MERS, and SARS in a nonhuman primate model. *Science* **368**(6494), 1012–1015 (2020)
23. Stokel-Walker, C.: What we know about Covid-19 reinfection so far. *BMJ* 372 (2021)